Electronic structure of Mn impurities in noble metals

D. van der Marel, C. Westra, and G. A. Sawatzky
Physical Chemistry Department of the Materials Science Center, University of Groningen, 9747-AG Groningen, The Netherlands

F. U. Hillebrecht
Institut für Festkörperforschung der Kernforschungsanlage Jülich, D-5170 Jülich, Federal Republic of Germany

(Received 24 September 1984)

Various electron-spectroscopy techniques are used to determine the electronic structure of Mn impurities in Ag and Cu. The spectral distributions of both minority- and majority-spin impurity d states are determined experimentally and compared to model calculations considering the photoemission matrix elements. The exchange and Coulomb integrals and energetic positions of the impurity d states as well as the impurity-host d-s and d-d hybridizations are determined. We find that the impurity minority-spin states are quite wide and lie close to the Fermi level, which raises questions concerning the validity of the use of a Kondo Hamiltonian to determine the low-energy scale properties. In addition, the hybridization of the majority-spin states with the host d band is larger, causing these to delocalize, whereas the magnetic moment remains localized. This large hybridization can introduce new exchange mechanisms not foreseen in conventional models.

I. INTRODUCTION

Mn dissolved in Ag and Cu form extensively studied systems of binary alloys. In 1951 dilute *Cu*Mn and *Ag*Mn were found to exhibit a resistivity minimum,[1] which, after the discovery of the now well-known Kondo divergency, led to a flurry of both experimental and theoretical activity. Later,[2] the same alloy systems were found to exhibit spin-glass behavior, which stimulated research in the more concentrated alloy systems. Because of the interesting properties of these materials, virtually the whole arsenal of experimental and theoretical techniques available to the solid-state physicist has been used to study these materials. The results obtained from these studies are discussed in several reviews.[3]

A very basic question, which is, up to now, still open, concerns the validity of using the Kondo Hamiltonian to describe the ground-state properties of these systems. The Kondo Hamiltonian describes the scattering of conduction electrons by a localized spin via an exchange interaction $J(k,k')$, and is of the form

$$H=-(2N)^{-1}\sum_{k,q}J_{kq}[\,S_z(c^{\dagger}_{q\uparrow}c_{k\uparrow}-c^{\dagger}_{q\downarrow}c_{k\downarrow}) +S_+c^{\dagger}_{q\downarrow}c_{k\uparrow}+S_-c^{\dagger}_{q\uparrow}c_{k\downarrow}]\,. \quad (1)$$

The Zeeman part of this Hamiltonian gives rise to the so-called Ruderman-Kittel-Kasuya-Yosida[4] (RKKY) spin-density oscillations around the magnetic impurity, which, in turn, leads to an oscillatory indirect-exchange interaction between impurities. This type of interaction is usually assumed in studies of the spin-glass behavior, and much work has been done to determine the strength of the exchange interaction. The spin-flip-scattering terms give rise to the Korringa-like linear temperature dependence of the linewidths in NMR and ESR experiments. In addition, the spin-flip-scattering parts result in a divergence in the perturbational treatment of the conduction-electron scattering at a characteristic temperature referred to as the Kondo temperature.

In using the Kondo Hamiltonian, one assumes that the impurity has no electronic degrees of freedom corresponding to energies in the vicinity of the ground state. In other words, the occupied impurity states must be far below the Fermi level and the unoccupied states must be far above the Fermi level. The only impurity degrees of freedom left then are of spin and/or orbital nature. This condition is derived in a more elegant manner by Schrieffer and Wolff,[5] who showed that the more general Anderson Hamiltonian could be transformed to a Kondo Hamiltonian provided that $r_{\pm}=\Gamma_{\pm}/|\varepsilon_{\pm}| \ll 1$, where $\Gamma_{\pm}$ and $\varepsilon_{\pm}$ are the width and energy, respectively, of the majority-spin $(+)$ and minority-spin $(-)$ states.

It should be noted that even if the above conditions do not hold, it may still be possible, in certain cases, to describe the system with a Kondo-like Hamiltonian. To see whether or not this is the case, one would have to study the higher-order terms of the Schrieffer-Wolff transformation.

As we will show below, it is probably inappropriate to try to describe Mn impurities with a Kondo Hamiltonian, suggesting the use of the more general Anderson Hamiltonian. The Anderson Hamiltonian[6] in its more general form reads

$$H=\sum_{k,\sigma}\eta_{k\sigma}c^{\dagger}_{k\sigma}c_{k\sigma}+\sum_{m,\sigma}\varepsilon_d d^{\dagger}_{m\sigma}d_{m\sigma}+\sum_{k,m,\sigma}V_{km}(d^{\dagger}_{m}c_{k\sigma}+c^{\dagger}_{k\sigma}d_m)+\sum_{\substack{i,j,\\k,l}}U(i,j,k,l)d^{\dagger}_i d_j d^{\dagger}_k d_l \ . \tag{2}$$

The last term describes the electronic structure of the impurity atom and consists essentially of two kinds of contributions.

(1) It describes the term splittings within the atom keeping the number of d electrons fixed (Hund's-rule coupling).

(2) It describes the Coulomb contribution to the energy required to remove or add an electron for each of the terms of the $n+1$ or $n-1$ states. In other words, it provides for the difference in the ionization potential and electron affinity for the atom. This form for the Anderson Hamiltonian is often approximated by

$$H_I=\tfrac{1}{2}(U-J)\sum_{\substack{m\neq n\\m,n}}d^{\dagger}_{m\sigma}d_{m\sigma}d^{\dagger}_{n\sigma}d_{n\sigma}+\tfrac{1}{2}U\sum_{m,n}d^{\dagger}_{m\sigma}d_{m\sigma}d^{\dagger}_{n\underline{\sigma}}d_{n\underline{\sigma}} \ . \tag{3}$$

In this approximation one neglects the orbital dependence of the Coulomb interaction, which is known, from atomic theory, to be of the same order as the spin dependence. This also is clearly demonstrated in metals by the Auger spectra of pure Cu (Ref. 7) and Pd impurities in Ag (Ref. 8). If the Coulomb part of the Hamiltonian could be approximated by Eq. (3), a d^8 configuration would consist of two states, namely a singlet and a triplet with a splitting of $2J$, whereas the Auger spectra show that the orbital splitting of the singlets and triplets is comparable to the singlet-triplet splitting.

The term splitting of the atomic d^n states determined by $U(i,j,k,l)$ in Eq. (2) can be expressed in terms of two Slater integrals, F^2 and F^4, while the monopole contribution to the Coulomb energy is F^0. Usually, it is assumed that the monopole contribution is the largest in metals, as it is for the free atom. It then would suppress large polarity fluctuations, stabilizing a state with a particular number of d electrons. The F^2 and F^4 integrals then contribute to the stabilization of a particular term of a d^n configuration, which, in most cases, is a magnetic state.

Upon placing such an atom in a metallic host, several things can happen. The hybridization term in Eq. (2) causes a mixing of the d^n states with $d^{n\pm1}$ states, and also, in higher orders, causes a mixing of the various terms within d^n, resulting eventually in a loss of the atomic characteristics, and leads to a nonmagnetic ground state. Another consequence of the metallic surroundings is that the atomic Coulomb interactions are screened. A large number of Auger-spectroscopy investigations of Cu, Ni, Ag, Pd, and impurities such as Ni and Pd in metals have shown that the monopole term (F^0) is strongly screened, whereas the higher-multipole terms (F^2 and F^4) are reduced by at most 20% from the free-atom values.[9] This is an extremely important observation for the understanding of transition-metal impurities in solids.

In addition to the approximate forms usually used for the Coulomb interactions in the Anderson Hamiltonian, one also usually assumes that the host-metal density of states is constant in the energy region of interest. For transition-metal impurities in noble-metal hosts, the high host-metal d density of states not far from the Fermi level might play an important role if these states hybridize sufficiently with the impurity d states. In this sense the noble-metal d bands are not unlike the ligand p bands in halides and chalcogenides, which are known to be the mediators for relatively strong superexchange interactions.

In an attempt to obtain more information about the relative importance of the above-mentioned interactions, we undertook a detailed investigation of *Cu*Mn and *Ag*Mn alloys. The aim of the investigation is to obtain information concerning (a) the energies of the majority- and minority-spin states of Mn, (b) the magnitude of the Mn d—host sp hybridization, (c) the importance of the Mn d—host d hybridization, and (d) the magnitude of the impurity d-d Coulomb interactions F^0, F^2, and F^4, which are related to U and J in frequently used approximations.

The experimental techniques used are x-ray photoelectron spectroscopy (XPS), x-ray-excited Auger spectroscopy (XAES), high-resolution ultraviolet photoelectron spectroscopy (UPS), and bremsstrahlung isochromat spectroscopy (BIS).

Before we present the results, it is useful to illustrate what we might hope to learn from these techniques. To do this, we consider the Mn impurity to be in its d^5 Hund's-rule ground state $d^5(^6S)$, as suggested by the experimentally determined magnetic moment, which is close to $5\mu_B$.[10] By the removal of one d electron, as in UPS, we can determine the energy of the d^4 states, of which only the $d^4(^5D)$ is accessible by fractional-parentage arguments. By the addition of one d electron, as in BIS, we can determine the energy of the d^6 states, of which, again, only the ^5D state is accessible. By careful data analysis, we should be able to determine the spectral distributions of these states from which the s-d and the impurity-host d-d hybridization can be determined. With Auger spectroscopy, we remove two d electrons, ending up in a d^3 configuration, of which only the ^4F and ^4P states are accessible.

From these measurements we can obtain the majority-spin "hole" energies, the minority-spin "electron" energies, and the Coulomb interactions. For the latter we proceed as follows:

$$\begin{aligned}&[E(d^6(^5D))-E(d^5(^6S))]-[E(d^4(^5D))-E(d^5(^6S))]=F^0+\tfrac{4}{14}(F^2+F^4)\ ,\\ &[E(d^3(^4F,^4P))-E(d^5(^6S))]-2[E(d^4(^5D))-E(d^5(^6S))]=F^0-\tfrac{1}{14}(F^2+F^4)\ ,\end{aligned} \tag{4}$$

as can be found in Slater's[11] treatment of term splittings, where $E(d^3(^4F,^4P))$ is the average energy. In this way, we have enough information to obtain F^0 and F^2+F^4. In the more conventional notation for magnetic impurities, F^0 is equivalent to U, and $\frac{1}{14}(F^2+F^4)=J$.

It is perhaps instructive at this point to briefly discuss the energetics of d^n configurations to remind the reader of the, in atomic physics, well-known energy-level diagram. We show in Fig. 1 all the atomic terms for the configurations $d^1 \rightarrow d^{10}$, as calculated using Slater's expressions for the term energies in terms of the F^0, F^2, and F^4 integrals. For F^0 we used 1.04 eV, and for the F^2 and F^4 integrals, 8.94 and 5.62 eV, which are reduced by 20% from the Mn free-atom values.[12] These are values which were determined from the present study as discussed below. The energy-level diagram is drawn assuming the $d^5(^6S)$ state to be the ground state. The point we want to make here is that the term energies of a d^5 configuration are spread over an 11-eV interval, which is an order of magnitude larger than the expected hybridization widths. Another important point concerns the "gap" of 3 eV seen in Fig. 1 between the Hund's-rule ground-state term and the first higher-energy term. It is this large gap which strongly favors a magnetic ground state.

II. EXPERIMENTAL SETUP

A. Instrumental details

Three different experimental setups were used for the study presented here. The XPS and XAES spectra were obtained with a modified AEI (KRATOS) ES200 spectrometer. Both Al and Mg $K\alpha$ x-ray sources were used. The base vacuum in the 10^{-11}-Torr range was obtained with turbine pumps and a liquid-nitrogen-cooled Ti sublimation pump. The sample-preparation chamber was equipped with Ar-ion-etching and sample-scraping capabilities.

The UPS measurements were done using a cylindrical mirror analyzer as described by Bosch.[13] The base pressure was in the 10^{-11}-Torr range, achieved with a combination of a diffusion pump and a liquid-nitrogen-cooled Ti sublimation pump. The samples could be argon-ion-etched and heat-treated *in situ*. The surface contamination was checked using electron-excited Auger spectroscopy using the same electron analyzer. The light source was a He resonance lamp operated to optimize the He I component. The energy resolution of the instrument was 40 and 80 meV at 5 and 10 eV pass energy, respectively.

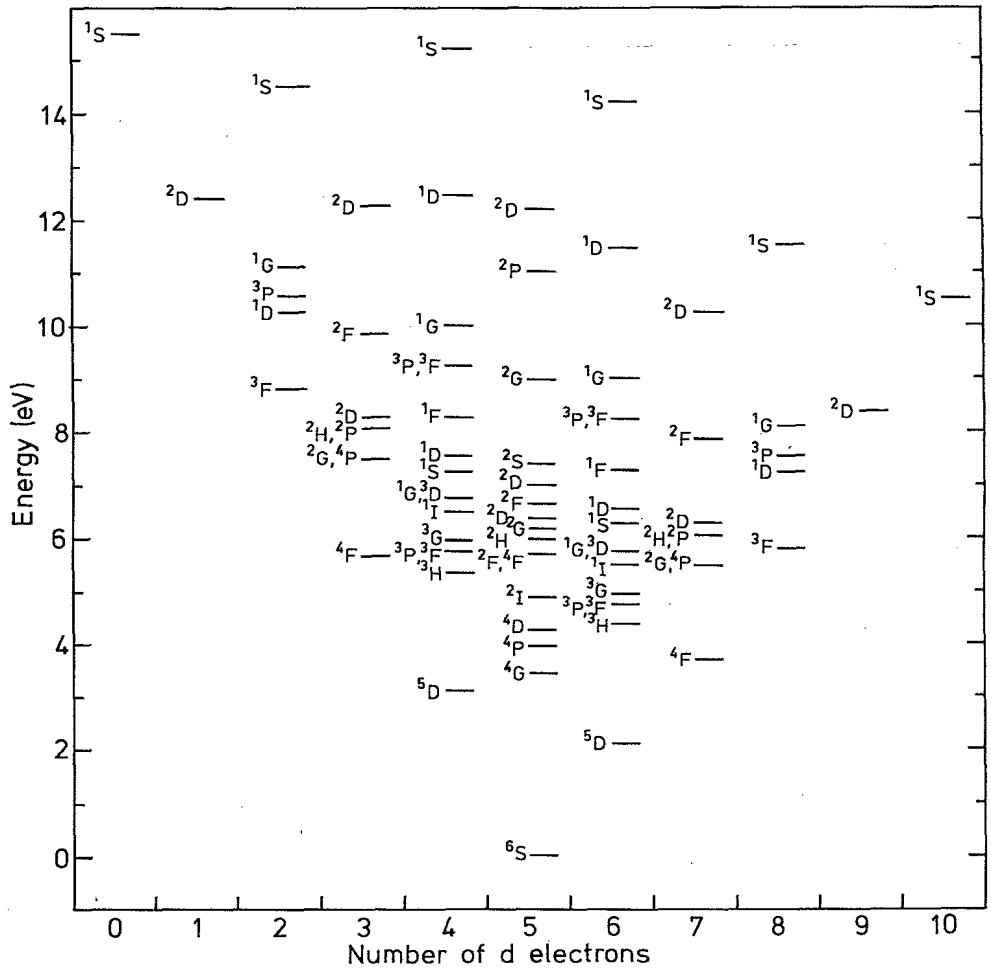

FIG. 1. Quasiatomic d states of a Mn atom in a Ag surrounding, calculated from Slater's atomic tables and using $I=-3.10$ eV, $F^0=1.04$ eV, $F^2=8.94$ eV, and $F^4=5.62$ eV.

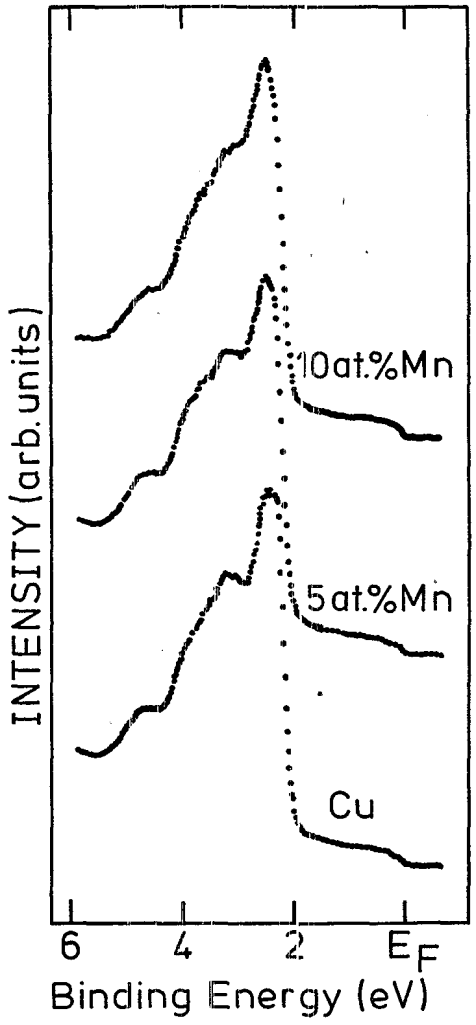

FIG. 2. UPS spectra of Cu, $Cu_{0.95}Mn_{0.05}$, and $Cu_{0.9}Mn_{0.1}$ dilute alloys.

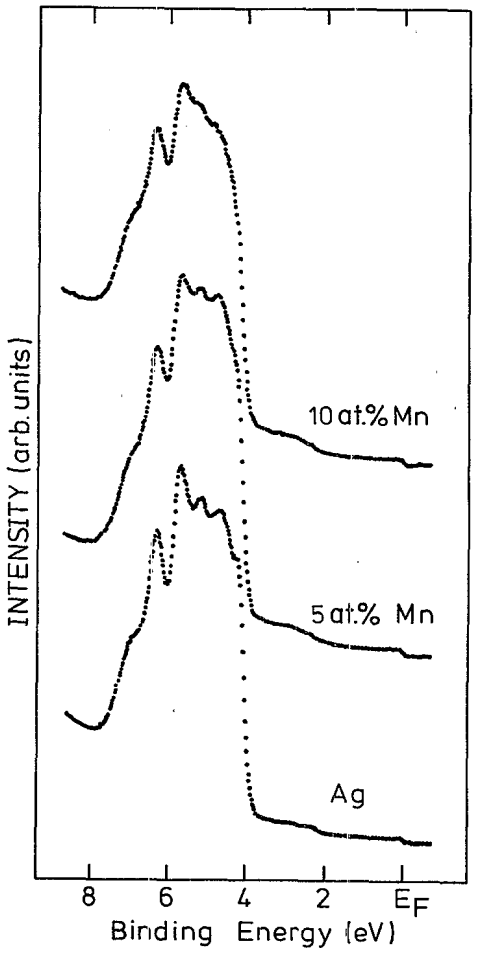

FIG. 3. UPS spectra of Ag, $Ag_{0.95}Mn_{0.05}$, and $Ag_{0.9}Mn_{0.1}$ dilute alloys.

In the cases presented here, we used 10 eV pass energy. To obtain sufficient statistics, multiple scans were accumulated with intermittent surface treatments every 30 min.

The BIS results were obtained with an instrument described elsewhere.[14] The base pressure was in the 10^{-11}-Torr range but increased to 10^{-10} Torr with the electron gun operating. Surface-contamination checks were done with XPS in the same instrument. Again, multiple scans were required to obtain sufficient statistics with intermittent sample scraping in the preparation chamber. The resolution as determined from the Fermi-edge cutoff in pure Ag and Cu was 0.85 eV.

B. Sample preparation

The polycrystalline *Ag*Mn samples (5 and 10 at.%) were obtained from the melt. Metallographic examinations showed that the samples were homogeneous and showed no secondary phases. The polycrystalline *Cu*Mn (1.5, 5, 10, and 15 at.%) samples were supplied by Mydosh and co-workers.[15] Although it is generally agreed that there is an anticlustering tendency in the otherwise random substitutional dilute alloys *Ag*Mn and *Cu*Mn, recent extended x-ray-absorption fine-structure (EXAFS) results[16] show 100% anticlustering for nearest-neighbor Mn atoms in *Ag*Mn up to 14 at.% impurity concentration. Diffuse x-ray-diffraction results[17] show 50 at.% Mn microdomains above 8 at.% impurity concentration, whereas neutron-scattering experiments[18] show only partial deviations from randomness in the first-neighbor shell. In addition, the double-peaked structures in the XPS measurements[19] on co-evaporated *Ag*Mn alloys by Höchst *et al.* indicate the presence of Mn clusters in the concentration range above 7 at.%. As we did not observe such features in the XPS spectra of our samples, we believe that the occurrence of Mn clusters is highly dependent on the details of sample preparation. We will assume that the Mn atoms in our samples can be considered diluted.

Another problem concerning the Mn concentration is related to the segregation enthalpy of Mn in Cu and Ag. From Miedema's tables[20] we obtained -0.16 and 0.12 eV for the segregation enthalpy of Mn in Cu and Ag, respectively. This would imply that equilibrium Mn surface concentration in a *Cu*Mn alloy is almost 100 at.% at room temperature. We checked the impurity concentrations of our samples after scraping and argon-ion etching

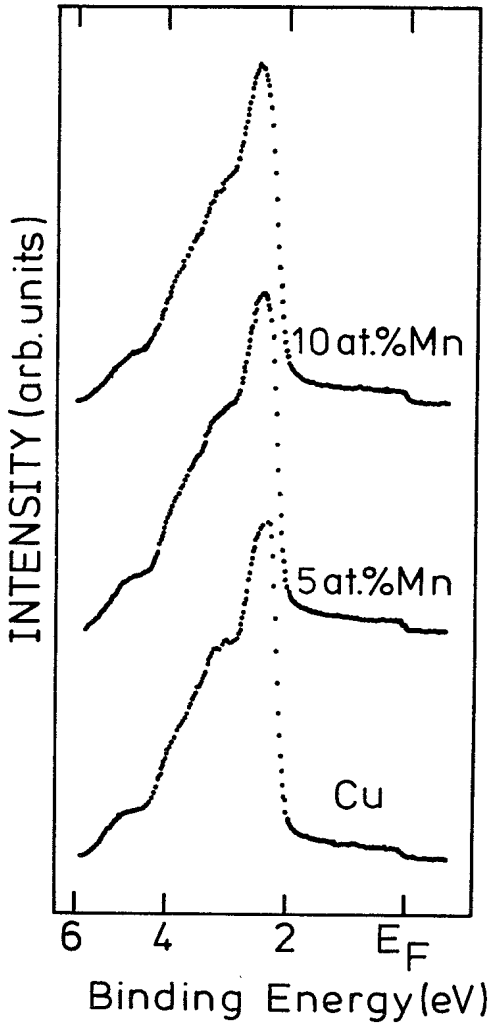

FIG. 4. UPS spectra of Cu, $Cu_{0.95}Mn_{0.05}$, and $Cu_{0.9}Mn_{0.1}$ dilute alloys corrected for a He I satellite, analyzer transmission, and inelastically scattered electrons.

in situ with electron-excited AES and XPS.

All the results showed that the Mn surface concentration was strongly enhanced in all *Ag*Mn and *Cu*Mn alloys immediately after insertion of the polished samples, and that the surface was strongly oxidized. However, as soon as an oxygen- and carbon-free surface was obtained, with either scraping or argon-ion etching, the cross-section-weighted Mn $2p$ lines, as compared to the host-core lines, had intensities close to those expected from the chemical composition.

III. RESULTS

In Figs. 2 and 3 we show the UPS spectra of the pure hosts and several concentrations of Mn in Ag and Cu. These spectra were subsequently corrected for the 23.08-eV He satellite and for a scattered-electron background. The He-satellite relative intensity was obtained from the Ni Fermi edge. The scattered-electron background was corrected for by using an iterative procedure.[21] In addition, we applied a $1/E$ correction[22] to the intensity to account for the energy-dependent transmission of our

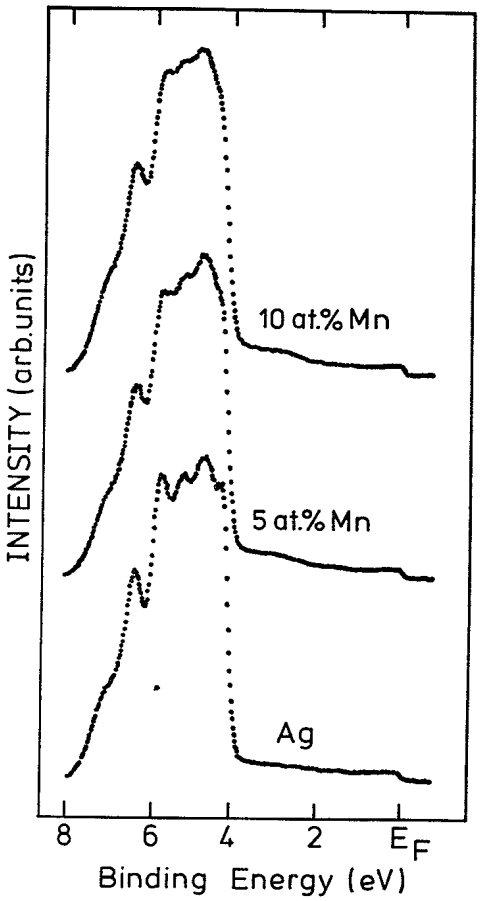

FIG. 5. UPS spectra of Ag, $Ag_{0.95}Mn_{0.05}$, and $Ag_{0.9}Mn_{0.1}$ dilute alloys corrected as in Fig. 4.

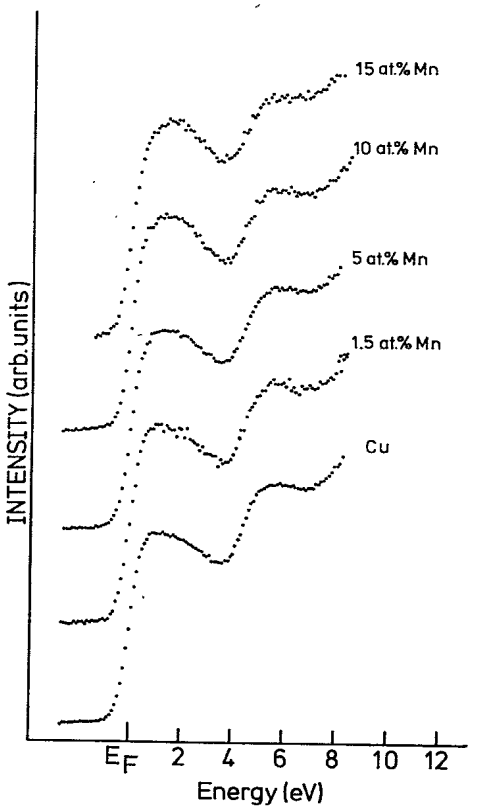

FIG. 6. *Cu*Mn BIS spectra.

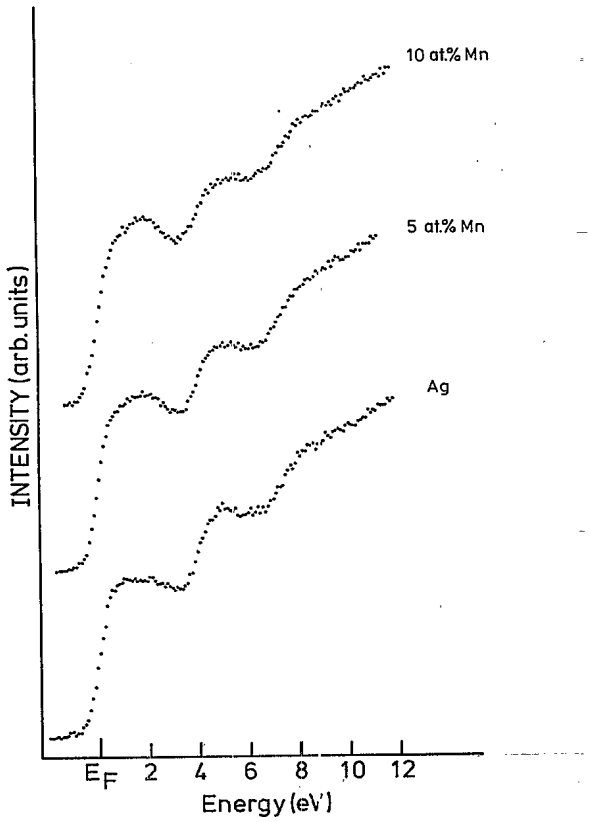

FIG. 7. *Ag*Mn BIS spectra.

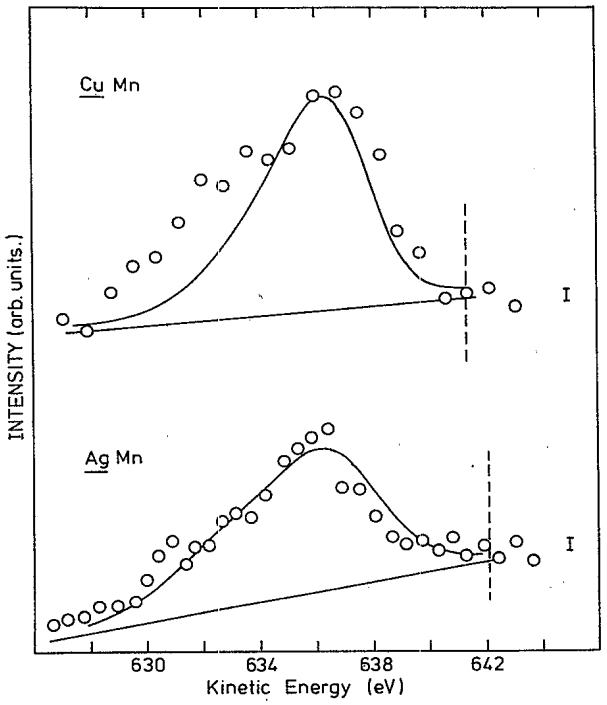

FIG. 9. $Cu_{0.9}Mn_{0.1}$ and $Ag_{0.95}Mn_{0.05}$ Mn L_3VV Auger spectra. Circles, experimental; solid lines, theoretical (see text). The vertical lines correspond to the Mn $2p_{3/2}$ XPS peak positions of Fig. 8, or, in different words, to the two-hole–excitation threshold.

analyzer. The so-obtained corrected spectra are shown in Figs. 4 and 5.

The BIS spectra shown in Figs. 6 and 7 have not been corrected in any way, since, at the high energies used, experience shows that the inelastic scattering background is not nearly as sensitive to the details of the surface as it is in UPS. Furthermore, the transmission in this relatively small energy range is nearly energy independent.

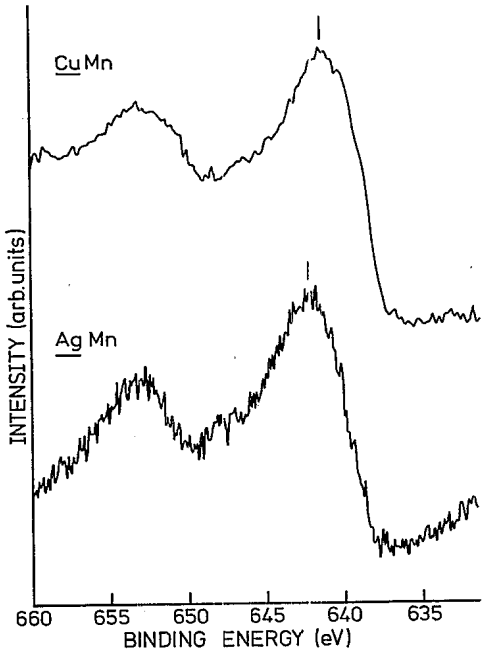

FIG. 8. $Cu_{0.9}Mn_{0.1}$ and $Ag_{0.95}Mn_{0.5}$ XPS spectra of the Mn $2p_{1/2,3/2}$ lines. The vertical bars indicate the energy positions used in the text.

The XPS and AES measurements were done on samples treated by both scraping and argon-ion etching. No detectable difference was observed in the spectra using these procedures. The spectra were obtained using both Al and Mg $K\alpha$ x-ray sources to avoid accidental overlap of Auger and photoelectron components. The Mn $2p$ XPS spectra are shown in Fig. 8, and the $L_{2,3}M_{4,5}M_{4,5}$ Auger spectra in Fig. 9. The Mn $2p$ binding energies and Auger kinetic energies are presented in Table I.

IV. DISCUSSION

The UPS spectra of *Ag*Mn alloys shown in Fig. 3 clearly exhibit a peak between the Ag d band and the Fermi level which we attribute to the majority-spin virtual bound state of Mn. Assuming that the ground state is close to $d^5(^6S)$, this peak would correspond to a $d^4(^5D)$ state. We note, however, that this state is quite close in energy to the Ag d band, so that hybridization herewith

TABLE I. Binding energies and average kinetic energies of Mn $2p_{3/2}$ XPS lines and L_3VV Auger transitions.

System	Mn $2p_{3/2}$ XPS binding energy (eV)	Mn L_3VV Auger kinetic energy (eV)
*Ag*Mn	642.2±0.5	635.3±0.5
*Cu*Mn	641.3±0.5	635.0±0.5

could be quite important. In the *Cu*Mn spectra this extra peak is not visible, which suggests that the Mn $d^4(^5D)$ state lies inside the Cu d band. This is also expected from energetic considerations. Assuming the d^4 state of Mn to be at about the same energy in Ag and Cu hosts, we see from the *Ag*Mn measurement that it will be close to the center of the Cu d band. This would result in strong mixing with the Cu d states.

In order to obtain a better picture of the changes in the host d-band structure, in Fig. 10 we present the difference spectra. These spectra were obtained by normalizing the surface under the spectra of Figs. 4 and 5 integrated up to E_F. The intensities of each normalized spectrum were then weighted with the average number of occupied d levels in the atomic state, and the intensities of the pure-metal spectra were subtracted from the weighted alloy spectra. It is assumed here that it is mainly the d part of the density of states that is observed in UPS.

In Fig. 10 we see several features that increase in intensity upon increasing the Mn concentration. In the *Ag*Mn spectra we observe a peak at 3.1 eV that is Lorentzian shaped at the low-binding-energy side and that broadens inhomogeneously as a function of Mn concentration, as in *Ag*Pt.[23] The small hump at 3.6 eV, very close to the Ag d-band edge, increases in intensity upon oxidation and seems to be due to a trace of Mn impurities in an oxidized state. We also see large changes in the host d-band density of states, with sharp structures occurring at energies where the pure-metal d-band density of states is strongly energy dependent. These changes are due to several discernable effects.

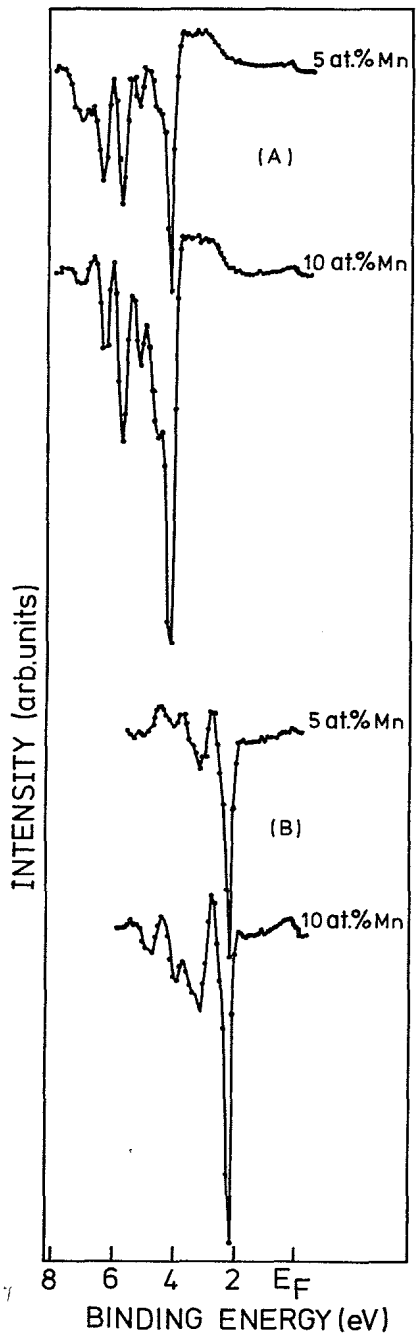

FIG. 10. Difference spectra of the (A) *Ag*Mn and (B) *Cu*Mn UPS spectra and the corresponding pure-metal spectra of Figs. 4 and 5. The 5- and 10-at. % alloy difference spectra are at an absolute scale relative to the pure-host—metal spectra. The solid lines serve as a guide to the eye.

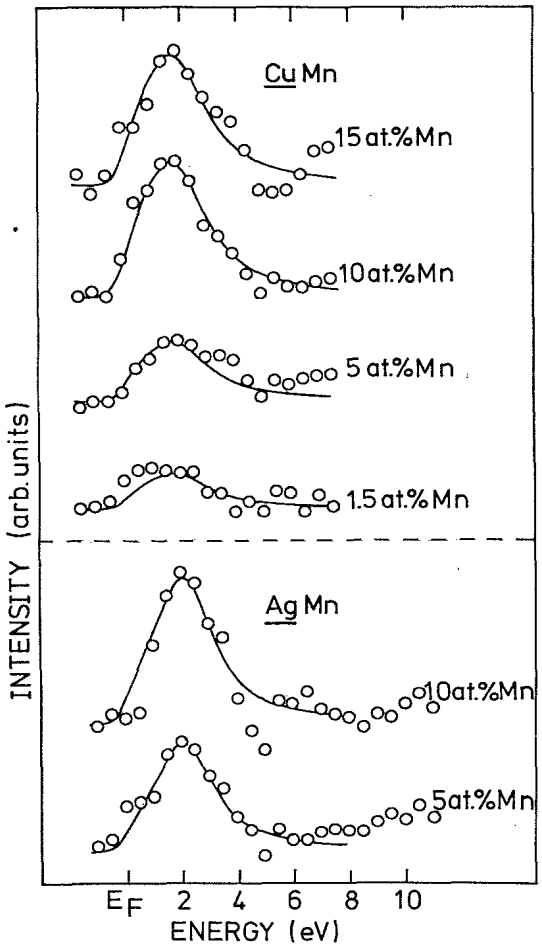

FIG. 11. Difference spectra of the *Ag*Mn and *Cu*Mn BIS spectra and the corresponding pure-metal spectra of Figs. 6 and 7. The intensities of the difference spectra are at an absolute scale relative to the pure-host-metal spectra.

We could consider the changes in electronic structure upon alloying as a three-step process. We first remove a Ag (Cu) atom, creating a vacancy with no d resonances in that energy range.[24] We now put in a Mn atom which has its d state just above the Ag d band broadened by the s-d hybridization. We then "turn on" the hybridization of these d states with the Ag d states. The d states on Ag atoms close to a Mn site will be pushed to somewhat higher binding energy, while those for Ag atoms far away will remain unchanged and some Mn d character will appear in the Ag d band. The net effect of this will be a negative contribution due to the removal of an Ag atom, a positive Mn d peak just above the Ag d band, a positive contribution in the Ag d band due to the Mn d character, and a contribution similar to the energy derivative of the Ag d-band density of states. We will show below that all these qualitative effects are nicely described by a more formal theory.

Since Mn has a large magnetic moment in Ag and Cu, not all the Mn d states can be full, yet we see a "gap" between the occupied d states and the Fermi level, suggesting that a subset of split-off states is full, which would correspond to a half-filled d shell. The other remaining Mn d states are observed above the Fermi level in the BIS spectrum (Figs. 6 and 7), in addition to steplike structures which are due to critical points[25] in the band structure. To see the Mn contribution more clearly, we show the difference spectra in Fig. 11. These spectra are obtained by normalizing the intensities at 10 eV to the same value and subtracting. At 10 eV we expect the influence of Mn to be negligible.

The difference spectra show only a peak just above the Fermi level which must correspond to the "missing" minority-spin d states of Mn. We notice that these are quite close to the Fermi level, which, as we will show below, has serious consequences for the use of a Kondo-like Hamiltonian. The intensity of this peak shows the same trend upon increasing the Mn concentration as the UPS spectra of Fig. 10. The solid line is a Lorentzian distribution with a sharp cutoff at the Fermi level. In order to make a direct comparison with the experimental spectra possible we convoluted this distribution with a Gaussian with a full width at half maximum (FWHM) of 0.85 eV corresponding to the experimental resolution in the BIS spectra. The positions and widths for the Lorentzian distribution are given in Table II.

Before going on to the other results, we would first like to analyze the UPS and BIS data in more detail in terms of a model Hamiltonian. For the model Hamiltonian we use a modified Clogston-Wolff[26] model to include the s-d hybridization and the large exchange splitting. This model treats the impurity d-host d hybridization in a simple, but in our case, realistic, manner. The majority-spin part (H_+) describes the ionization spectrum and the minority-spin part (H_-) describes the affinity spectrum, assuming the ground state to be $d^5(^6S)$. The Hamiltonian is written as

$$H=\sum_\sigma \left[\sum_{\mathbf{k}} \varepsilon_{\mathbf{k}} d^\dagger_{\mathbf{k}\sigma} d_{\mathbf{k}\sigma} + \sum_l \eta_l c^\dagger_{l\sigma} c_{l\sigma} + \Delta_{d\sigma} d^\dagger_{0\sigma} d_{0\sigma} + \sum_l V_{ld} (d^\dagger_{0\sigma} c_{l\sigma} + c^\dagger_{l\sigma} d_{0\sigma}) \right] . \quad (5)$$

Here, $\varepsilon_{\mathbf{k}}$ describes the energy dispersion of the host d band, η_k that of the s band, $\Delta_{d\sigma}=E^i_{d\sigma}-\bar{\varepsilon}_d$ the average impurity d-state energies relative to the d-band centroid, and V_{kd} the hybridization of the impurity d state with the sp band. The impurity d—host d hybridization is included implicitly, and the assumption is made that the impurity d wave function is identical to that of the host, but its energy is shifted. In this mode the d-d Coulomb interactions do not appear explicitly, but are incorporated in the energy difference $\Delta_{d+}-\Delta_{d-}$. This approximate treatment of the Coulomb interactions is reminiscent of a spin-polarized Hartree-Fock calculation. In writing the Hamiltonian in this way, we assume that H_+ commutes with H_-, which neglects all possible spin-flip processes and the influence of higher-energy terms present in the impurity atom's electronic structure (see Fig. 1). The spin-flip processes are, of course, of utmost importance to describe the Kondo properties. We, however, expect these to be important only very close to the Fermi level, and to have no significant influence on the larger-energy-scale properties. The above approximate manner of including Coulomb and exchange interactions will be valid only if

TABLE II. Experimental (footnotes a and b) and theoretical (footnotes c—e) values for the minority- and majority-spin peak positions and widths of *Ag*Mn and *Cu*Mn.

System	ε_+ (eV)	Γ_+ (eV)	r_+	ε_- (eV)	Γ_- (eV)	r_-
*Ag*Mn[a]	−3.1±0.2	0.7±0.1	0.23	2.1±0.2	1.2±0.1	0.57
*Ag*Mn[b]	−3.25			1.6		
*Ag*Mn[c]	−2.6[f]	0.2[f]	0.07	0.7[f]	0.6[f]	0.86
*Cu*Mn[a]				1.7±0.2	1.4±0.2	0.82
*Cu*Mn[d]				0.79[f]	0.8[f]	1.01
*Cu*Mn[e]	−3.5[f]	0.16[f]	0.05	0.8[f]	0.64[f]	0.8

[a]This work.
[b]Reference 30.
[c]Reference 32.
[d]Reference 29.
[e]Reference 31.
[f]Estimated from the figures.

the ground state is close to $d^5(^6S)$, which we know is true for Mn impurities in Ag and Cu.

Having made these approximations, we have reduced the problem to that of the sum of two one-particle problems, which is easily solved. Using the Dyson equation, the local-impurity density of states is given by

$$\pi^{-1}\mathrm{Im}\sum_{\sigma} G_{d0\sigma}^{d0\sigma} = \rho_{d0} , \tag{6}$$

where

$$G_{d0\sigma}^{d0\sigma} = g_{d0\sigma}^{d0\sigma} + g_{d0\sigma}^{d0\sigma}\Delta_{d\sigma}G_{d0\sigma}^{d0\sigma} + g_{d0\sigma}^{d0\sigma}\sum_{\mathbf{k}} V_{\mathbf{k}d}G_{s\mathbf{k}\sigma}^{d0\sigma} \tag{7}$$

and

$$G_{s\mathbf{k}\sigma}^{d0\sigma} = f_{\mathbf{k}\sigma}^{\mathbf{k}\sigma}V_{\mathbf{k}d}G_{d0\sigma}^{d0\sigma} , \tag{8}$$

or

$$G_{d0\sigma}^{d0\sigma} = \frac{g_{d0\sigma}^{d0\sigma}}{1-\left[\Delta_{d\sigma}+\sum_{\mathbf{k}}(V_{\mathbf{k}d})^2 f_{\mathbf{k}\sigma}^{\mathbf{k}\sigma}\right]g_{d0\sigma}^{d0\sigma}} . \tag{9}$$

Furthermore,

$$g_{d0\sigma}^{d0\sigma} = \sum_{\mathbf{k}} \frac{1}{\omega-\epsilon_{\mathbf{k}}}$$

is the host d-band density of states, and

$$f_{\mathbf{k}\sigma}^{\mathbf{k}\sigma} = \frac{1}{\omega-\eta_{\mathbf{k}}}$$

describes the s-band density of states. To simplify matters, we further assume that $(V_{\mathbf{k}d})^2$ can be replaced by its average value, and that the host s-band density of states is constant in the relevant energy region so that

$$\sum_{\mathbf{k}}(V_{\mathbf{k}d})^2 f_{\mathbf{k}\sigma}^{\mathbf{k}\sigma} \simeq i\Gamma_{\sigma} , \tag{10}$$

$$G_{d0\sigma}^{d0\sigma} = \frac{g_{d0\sigma}^{d0\sigma}}{1-(\Delta_{d\sigma}+i\Gamma_{\sigma})g_{d0\sigma}^{d0\sigma}} . \tag{11}$$

Obviously, our difference spectra do not correspond to the local-impurity density of states, which is positive everywhere. This is also expected since the host density of states will also be modified. We therefore also calculate the total density of states:

$$\rho_d(\mathrm{tot}) = \pi^{-1}\mathrm{Im}\sum_{\mathbf{k},\sigma} G_{d\mathbf{k}\sigma}^{d\mathbf{k}\sigma} . \tag{12}$$

The Dyson equation gives

$$G_{dq\sigma}^{d\mathbf{k}\sigma} = g_{dq\sigma}^{dq\sigma}\delta_{\mathbf{k}q} + g_{dq\sigma}^{dq\sigma}\frac{\Delta_{d\sigma}}{N}\sum_{m} G_{dm\sigma}^{dm\sigma} + g_{dq\sigma}^{dq\sigma}\sum_{l}\frac{V_{ld}}{\sqrt{N}}G_{sl\sigma}^{d\mathbf{k}\sigma} , \tag{13}$$

$$G_{sl\sigma}^{d\mathbf{k}\sigma} = f_{l\sigma}^{l\sigma}V_{ld}\sum_{m}\frac{1}{\sqrt{N}}G_{dm\sigma}^{d\mathbf{k}\sigma} , \tag{14}$$

$$G_{dq\sigma}^{d\mathbf{k}\sigma} = g_{dq\sigma}^{dq\sigma}\delta_{q\mathbf{k}} + g_{dq\sigma}^{dq\sigma}\left[\frac{\Delta_{d\sigma}+i\Gamma_{\sigma}}{N}\right]\sum_{m} G_{dm\sigma}^{d\mathbf{k}\sigma} , \tag{15}$$

or

$$G_{d\mathbf{k}\sigma}^{d\mathbf{k}\sigma} = g_{d\mathbf{k}\sigma}^{d\mathbf{k}\sigma} + \frac{1}{N}\left[\frac{(\Delta_{d\sigma}+i\Gamma_{\sigma})(g_{d\mathbf{k}\sigma}^{d\mathbf{k}\sigma})^2}{1-\frac{\Delta_{d\sigma}+i\Gamma_{\sigma}}{N}\sum_{\mathbf{k}} g_{d\mathbf{k}\sigma}^{d\mathbf{k}\sigma}}\right] , \tag{16}$$

$$\Delta\rho_d(\mathrm{tot}) = -\pi^{-1}\mathrm{Im}\sum_{\sigma}\frac{(\Delta_{d\sigma}+i\Gamma_{\sigma})\frac{\partial}{\partial\omega}\frac{1}{N}\sum_{\mathbf{k}}\frac{1}{\omega-\epsilon_{\mathbf{k}}}}{1-(\Delta_{d\sigma}+i\Gamma_{\sigma})\frac{1}{N}\sum_{\mathbf{k}}\frac{1}{\omega-\epsilon_{\mathbf{k}}}} , \tag{17}$$

where $\Delta\rho_d(\mathrm{tot})$ is the change in the density of states in the dilute limit. We notice that the total change in the d density of states contains a derivative which results in the sharp structures seen in Fig. 10.

A difficulty with this expression is that $\Delta\rho_d(\mathrm{tot})$ is not zero for $\Delta=0$ as it should be, since in a calculated band structure the s-d hybridization is already included. The term remaining involving $i\Gamma$, however, introduces a negligible error for the values of Γ which we require to give the experimental virtual-bound-state widths.

A direct comparison of experiment and theory can, however, only be made after inclusion of the photoemission matrix elements. For Ag and Cu these matrix elements are not constant over the host d band, and, in addition, the matrix element for Mn d photoemission can be considerably different from that of Ag and, to a lesser degree, Cu. In the Appendix we have derived an expression for the matrix-element effects following closely the arguments of Shevchik,[27] but including non-k-conservation in the initial state. From this we see that if the atomic cross sections for guest and host atoms are the same, we can write

$$\Delta\rho_d(\mathrm{tot}) = -\pi^{-1}\mathrm{Im}\left[\frac{\Delta(\partial/\partial\omega)g_{\mathrm{exp}}(\omega)}{1-\Delta g_0^0(\omega)}\right] , \tag{18}$$

where $g_{\mathrm{exp}}(\omega)$ is obtained from the pure-host UPS spectrum, i.e.,

$$I_d(\omega) = \pi^{-1}\mathrm{Im}[g_{\mathrm{exp}}(\omega)] . \tag{19}$$

In this way we can include, purely experimentally, the matrix-element effects within the host d bands. By including the matrix elements in this way, we should be able to make a fairly detailed comparison with experiment.

In Fig. 12 we compare the calculated spectrum to the experimental difference spectrum. The values of $\Delta_{\pm}$ and $\Gamma_{\pm}$ are chosen to give the correct peak positions and widths, and for $g_0^0(\omega)$ we use the semiempirical density of states as calculated by Smith.[28] The large experimental linewidth of the BIS part was included in the theory by convoluting the part above the Fermi level with a Gaussian of FWHM 0.85 eV. We see that the above-described theory follows the experimental curve surprisingly well.

To demonstrate the influence of the energy-dependent matrix-element effects, we also show, in Fig. 13, the calculated difference density of states [Eq. (17)] using the same parameters as for the curves of Fig. 12. Clearly, the theory including the matrix-element effects gives a much better representation of the spectrum. The peak positions as well as the relative intensities of the oscillations in the

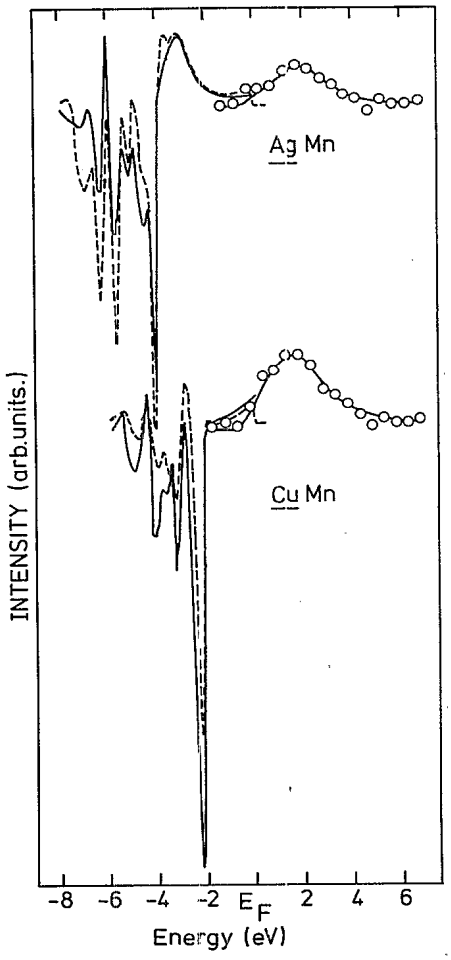

FIG. 12. Experimental and theoretical UPS and BIS difference spectra of $Cu_{0.9}Mn_{0.1}$ and $Ag_{0.95}Mn_{0.05}$. Dashed lines and circles, experimental spectra; solid lines, theoretical spectra.

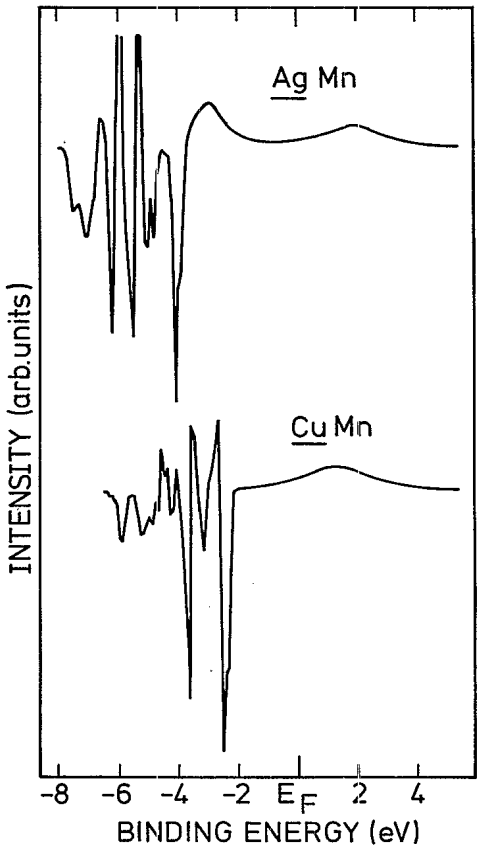

FIG. 13. Calculated difference density of states of *Ag*Mn minus Ag, and of *Cu*Mn minus Cu.

d band are strongly modified by matrix-element effects. In this theory we have assumed equal cross sections for Mn and host d emission. This is probably not valid for *Ag*Mn, but we notice from Eq. (A12) in the Appendix that the influence of a different cross section ($\gamma \neq 0$) for host and guest atoms does not effect the term involving the derivative of the density of states, and merely adds an only slowly-varying energy-dependent contribution in the host d band and a small modification of the intensity of the impurity line.

The parameters used to obtain the simulation in Fig. 12 are given in Table III. We notice that Δ_{d+} for *Cu*Mn is zero, placing the Mn majority-spin state in the center of the Cu d band, which, as we will see below, causes the local-impurity density of states to spread out over the whole Cu d band.

Having obtained the parameters, we can now calculate the local-impurity density of states using Eq. (11). This is shown in Fig. 14. We see, from this, the large influence of the Mn d-host hybridization, especially for the majority-spin states. For *Cu*Mn the impurity majority-spin d states are delocalized over the whole Cu band.

By integrating up to the Fermi level, we can also determine the occupation of the majority- and minority-spin states, as given in Table III, and the magnetic moment. We find $P_{\text{eff}} = 4.8\mu_B$ and $4.7\mu_B$, respectively, for *Cu*Mn and *Ag*Mn, which agree well with magnetic-susceptibility measurements.[10] We also see from Fig. 14 that the Mn minority-spin states are quite close to the Fermi level and have a considerable width. This suggests that the use of a Kondo Hamiltonian for describing the low-energy-scale properties is not appropriate. As discussed in the Introduction, the Schrieffer-Wolff transformation is only valid for $r_\pm = \Gamma_\pm / \varepsilon_{d\pm} \ll 1$, which certainly is not the case for these systems. The values of $r_\pm$ are given in Table II, from which we see that r_- is between 0.5 and 1.

In Table II we also give the experimentally determined

TABLE III. Parameters used in the model calculations. P_{eff} is obtained using $P_{\text{eff}} = g\sqrt{S(S+1)}$, with $S = \frac{1}{2}(n_+ - n_-)$. $n_\pm$ are the occupancies of the majority- and minority-spin impurity d states.

System	Δ_{d+} (eV)	Γ_+ (eV)	n_{d+}	Δ_{d-} (eV)	Γ_- (eV)	n_{d-}	P_{eff}
*Ag*Mn	2.2±0.1	0.7±0.1	4.44±0.1	7.3±0.2	1.2±0.1	0.77±0.1	4.6
*Cu*Mn	0	0	5	4.7±0.2	1.4±0.1	1.09±0.1	4.8

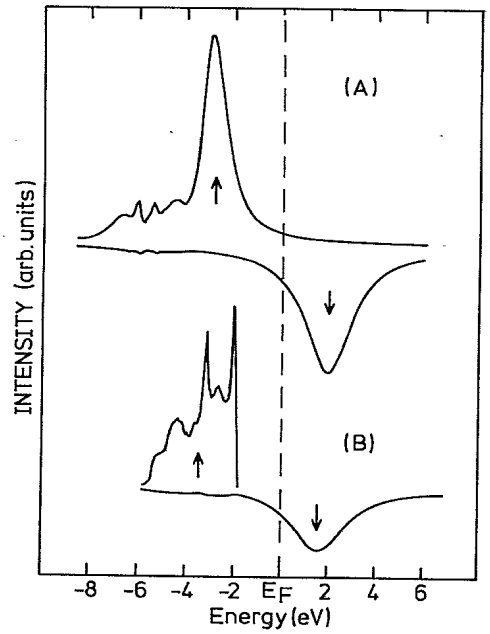

FIG. 14. Calculated spin-projected local d density of states at a Mn site in a (A) Ag and (B) Cu surrounding.

widths and positions of the impurity states, together with values from other investigations. We notice that the splitting between the majority- and minority-spin states, as determined here (5.3 eV for *Ag*Mn), is considerably larger than that obtained from first-principles calculations (3.5 eV).[29]

As described in the Introduction, we can obtain the Coulomb interactions from the minority- and majority-spin Mn d-state energies. From these, we obtain $F^0+\frac{4}{14}(F^2+F^4)=5.2$ eV for *Ag*Mn. To obtain the separate contributions of $F^0=U$ and the exchange $J=\frac{1}{14}(F^2+F^4)$, we can use the Auger results. The Auger spectra of Fig. 9 should, in the atomic limit, consist of two lines corresponding to $d^3(^4F)$ and $d^3(^4P)$ for an initial $d^5(^6S)$ ground state. However, as has recently been shown by Vos *et al.*,[8] the impurity Auger spectra are strongly distorted in nobel metals because of hybridization with the host-metal d states. The expected ^4F-^4P splitting will therefore not be observed, and we can use only the term average energy to estimate the Coulomb interactions. The average kinetic energy of the Auger electron is given by

$$E_{\rm kin}(^4F,^4P)=E_{2p_{3/2}}-E(d^3(^4F,^4P))\ ,$$

where $E_{2p_{3/2}}$ is the binding energy of the $M_{2p_{3/2}}$ electron. Using the values of Table I, we find $E(d^3(^4F,^4P))=(6.8\pm0.7)$ eV for *Ag*Mn, and using Eq. (4) we find $F^0-\frac{1}{14}(F^2+F^4)\simeq(0.0\pm0.7)$ eV, and using the UPS and BIS results we finally obtain $F^0\simeq(1.0\pm0.7)$ eV and $\frac{1}{14}(F^2+F^4)\simeq(1.0\pm0.2)$ eV. We see from these estimates that F^0 is strongly reduced from the free-atom value (22 eV),[11] a result which is quite general for $3d$ transition metals.[8] The higher-multipole terms in the Coulomb interaction, F^2 and F^4, remain close to the atomic value, $\frac{1}{14}(F^2+F^4)=1.2$ eV.[11] This also is a quite general result for the transition metals.[8] The solid lines in Fig. 9 are theoretical impurity Auger spectra obtained in the way described by Vos *et al.*,[8] starting from the local-impurity majority-spin DOS of Fig. 14. For the details of the calculation, we refer to Ref. 8. From the values for F^0, F^2, and F^4, we obtain $U_{\rm eff}(^4P)=1.3$ eV and $U_{\rm eff}(^4F)=-0.6$ eV for Mn in Ag, as can also be verified from Fig. 1. For Mn in Cu we took 0.7 and -1.2 eV respectively, assuming the same term splitting as in the Ag host, but a smaller F^0 value of about 0.4 eV.

Upon comparing the theoretical and experimental *Cu*Mn LVV spectra, we see that, experimentally, there is some more intensity at about 631 eV kinetic energy. We believe that this is caused by a slight oxidation of the Mn atoms during the measurement, as the intensity in this region was somewhat enhanced several hours after initial cleaning of the sample. However, also in the higher-kinetic-energy regions of the spectrum there are differences between the experimental and the theoretical line shape which may be very well due to the presence of the Mn minority-spin states close to the Fermi level. In the presence of a core hole, these states may become partially occupied, and the implicit assumption of initially full shells in the Auger process is no longer justified. An exact theory that takes into account such effects is, however, not available at present.

The above-mentioned values of F^0, F^2, and F^4, in addition to the UPS d^4 final-state energy, were used to generate the term energy diagram in Fig. 1. This diagram shows that the most important excited states mixed into the ground state because of hybridization with the sp bands are the $d^6(^5D)$ and $d^4(^5D)$ states. It is interesting that these states are also both magnetic, so that the mixing will not destroy the local moment.

From the above analysis we have obtained a fairly good picture of the electronic structure of these alloys, at least for the so-called high-energy-scale region. We already pointed out that the Clogston-Wolff-like theory used is not valid to describe the low-energy-scale region and therefore cannot be expected to be correct at the Fermi level. The high-energy-scale results, however, can now be used to do a more sophisticated calculation of the low-energy-scale properties. We notice from Fig. 1 that the most important configurations which will mix via s-d hybridization with the $d^5(^6S)$ state are the $d^6(^5D)$ and $d^4(^5D)$ states. Of secondary importance are the $d^5(^4G,^4P,^4D)$ states which can mix in higher orders in V_{kd} via the $d^6(^5D)$ and $d^4(^5D)$ states. We also notice that the $d^6(^5D)$ and $d^4(^5D)$ states are both fivefold orbitally degenerate, which is sufficiently large to expect a fast convergence of a $(1/N)$-type perturbation expansion.[33]

The Kondo Hamiltonian has been extensively used to describe the exchange interaction between magnetic impurities leading to the well-known RKKY oscillatory behavior thereof. The above results raise serious questions concerning the validity of such an approach for two reasons. First, the validity of the use of the Kondo Hamiltonian is questionable, and, second, the Mn d-host d hybridization, which we find to be strong, is not included in the RKKY theory. The most extreme cases are the majority-spin states in *Cu*Mn, which are apparently delo-

calized over the entire Cu d band. This strong delocalization is also present, to a lesser extent, in *Ag*Mn. The minority-spin Mn states can, on the other hand, be considered to be quite localized, although even these have some density in the host-metal d band. As a result the magnetic *moments* are localized at the Mn atoms, but the *d electrons* are not. A consequence of this is that d electrons also mediate exchange interactions between local moments. We see that there are two extensions of the usual RKKY interaction[4] to be made:

(1) The Anderson Hamiltonian must be used instead of the Kondo Hamiltonian.

(2) The occupied d bands of the host material must be included.

V. CONCLUSIONS

From this study we have obtained the following:

(1) A direct determination of the energy and widths of the impurity majority- and minority-spin states in *Cu*Mn and *Ag*Mn.

(2) The host d band is strongly perturbed by the impurity, which is well described by a modified spin-polarized Clogston-Wolff mode.

(3) The majority-spin impurity states are strongly delocalized via hybridization with the host d band. The minority-spin states remain quite localized.

(4) The close proximity of the minority-spin impurity state to the Fermi level, together with its large width, indicates that the use of a Kondo-like Hamiltonian to describe these systems is not appropriate.

(5) The monopolelike impurity d-d Coulomb interaction is strongly reduced from the free-atom value, whereas the higher-multipole terms are close to the atomic values.

(6) The host-metal d band could be an important mediator for superexchange-like interactions between impurity spins.

ACKNOWLEDGMENTS

This investigation was supported in part by the Netherlands Foundation for Chemical Research (SON) with financial aid from the Netherlands Organization for the Advancement of Pure Research (ZWO). Two of us, (D.v.d.M. and G.A.S.), would like to thank the Kernforschungsanlage Jülich for financial support and hospitality during their stay in Jülich.

APPENDIX

In general, the photoemission current can be written as

$$J(E,\Omega)=\sum_{k_f}{}'\sum_{k,g}\sum_{\mu,\nu}\{M_{k_f,q,\mu}M^{*}_{k_f,k,\nu}\mathrm{Im}[G^{k\nu}_{q\mu}(E-\Omega)]\}\ , \tag{A1}$$

where Ω is the photon energy, E the energy of the outgoing electron, and $M_{k_f,q,\mu}$ the transition matrix element to a state k_f from a state in band μ with wave vector q. The summation over k_f is limited to the constant-energy surface E. $G^{k\nu}_{q\mu}$ is the Green's function for the alloy.

Following Shevchik, (27) we write

$$M_{k_f,q,\nu}=\frac{1}{N}\sum_{n}e^{i(\mathbf{k}_f-\mathbf{q})\cdot\mathbf{R}_n}\sigma_n(k_f,\nu)\ , \tag{A2}$$

with the summation running over the atomic positions R_n, and

$$\sigma_n(k_f,\nu)=\sqrt{N}\,\langle\Psi_{k_f}\,|\,\mathbf{A}\cdot\mathbf{p}\,|\,\Psi_{\nu n}\rangle\ . \tag{A3}$$

In this expression we have used a Wannier representation of the initial-state wave functions and have assumed that the Wannier functions are wave-vector independent as, for example, in a tight-binding model. The cross section σ_n will depend only on the kind of atom on site n, the initial-state symmetry ν, and the final-state wave function. In the case of a pure material, σ is site independent, so that

$$M_{k_f,q,\nu}=\sigma(k_f,\nu)S(\mathbf{k}_f-\mathbf{q})\ , \tag{A4}$$

where $S(k)$ is the form factor given by

$$S(\mathbf{k})=\frac{1}{N}\sum_{n}e^{i\mathbf{k}\cdot\mathbf{R}_n}=\sum_{Q}\delta_{\mathbf{k},\mathbf{Q}}\ , \tag{A5}$$

where $\mathbf{Q}$ is a reciprocal-lattice vector.

For a single impurity at site $R_n=0$, we define

$$\gamma=(\sigma_{\mathrm{imp}}-\sigma_{\mathrm{host}})/\sigma_{\mathrm{host}}\ , \tag{A6}$$

and we will assume that γ is independent of k_f, and that the final-state wave function is not changed by the presence of the impurity. We then obtain

$$M_{k_f,q,\nu}=\sigma(k_f,\nu)[S(\mathbf{k}_f-\mathbf{q})+\gamma/N]\ , \tag{A7}$$

and, from Eq. (A1),

$$J(E,\Omega)=\mathrm{Im}\left[\sum_{k_f}{}'\sum_{\mu,\nu}\sigma(k_f,\mu)c^{*}(k_f,\nu)\left[G^{k_r}_{k_r}(E-\Omega)+2(\mathrm{Re}\gamma_\nu)\frac{1}{\sqrt{N}}G^{0\nu}_{k_r\mu}(E-\Omega)+\gamma_\mu\gamma^{*}_\nu\frac{1}{N}G^{0\nu}_{0\mu}(E-\Omega)\right]\right]\ , \tag{A8}$$

where k_r is k_f minus a reciprocal-lattice vector, and it lies in the first Brillouin zone. G^0_0 refers to the impurity Green's function.

We first consider the case studied by Shevchik, namely that the initial-state wave functions are unchanged by the impurity and only the cross sections are different for impurity and host. This is equivalent to

$$G^k_k=g^k_k,\ \ G^0_k=(1/\sqrt{N})g^k_k,\ \text{and}\ G^0_0=(1/N)\sum_k g^k_k\ , \tag{A9}$$

and

$$J(E,\Omega)=\mathrm{Im}\left[\sum_k{}' \,|\sigma|^2[g_k^k+2(\mathrm{Re}\gamma)cg_k^k+|\gamma|^2cg_0^0]\right]$$
$$=\mathrm{Im}\left[|\bar{\sigma}|^2\left[\sum_k{}' g_k^k(E-\Omega)\right]+\langle|\Delta\sigma|^2\rangle\sum_k g_k^k(E-\Omega)\right], \tag{A10}$$

with $C=1/N$, g_k^k the pure-host Green's function, and

$$|\bar{\sigma}|^2=\left|\frac{1}{N}\sum_i\sigma_i\right|^2=|\sigma_h|^2(1+2\gamma c)+O(1/N^2)\,,\quad \langle|\Delta\sigma|^2\rangle=\frac{1}{N}\sum_i|\sigma_i-\bar{\sigma}|^2=|\sigma_h|^2\gamma^2c+O(1/N^2)\,, \tag{A11}$$

which is the same result as obtained by Shevchik. To obtain the relation used in this paper [Eq. (18)], we substitute into Eq. (A8) the expressions for the Green's functions based on the Clogston-Wolff model, Eqs. (12)—(17),

$$J(E,\Omega)=\mathrm{Im}\sum_{k_f}{}'\left[|\sigma(k_f)|^2\left[g_{k_r}^{k_r}(E-\Omega)+\frac{1}{N}\frac{(\Delta+i\Gamma)[g_{k_r}^{k_r}(E-\Omega)]^2}{1-(\Delta+i\Gamma)g_0^0(E-\Omega)}+\frac{2}{N}(\mathrm{Re}\gamma)\frac{g_{k_r}^{k_r}(E-\Omega)}{1-(\Delta+i\Gamma)g_0^0(E-\Omega)}\right.\right.$$
$$\left.\left.+\frac{1}{N}|\gamma|^2\frac{g_0^0(E-\Omega)}{1-(\Delta+i\Gamma)g_0^0(E-\Omega)}\right]\right]. \tag{A12}$$

Taking $\gamma=0$ we obtain

$$J_{\mathrm{diff}}(E,\Omega)=\mathrm{Im}\sum_{k_f}{}'\left[|\sigma(k_f)|^2\frac{(\Delta+i\Gamma)[g_{k_r}^{k_r}(E-\Omega)]^2}{1-(\Delta+i\Gamma)g_0^0(E-\Omega)}\right], \tag{A13}$$

or

$$J_{\mathrm{diff}}(E,\Omega)=-\mathrm{Im}\frac{(\Delta+i\Gamma)(\partial/\partial\Omega)g_{\mathrm{exp}}(E-\Omega)}{1-(\Delta+i\Gamma)g_0^0(E-\Omega)}\,, \tag{A14}$$

where

$$\pi^{-1}\mathrm{Im}[g_{\mathrm{exp}}(E,\Omega)]=J_{\mathrm{host}}(E,\Omega)=\sum_{k_f}{}'|\sigma(k_f)|^2\delta(E-\Omega-\varepsilon_{k_r})\,,$$

and the real part is determined by the Kramers-Kronig transformation over Ω. In order to do this transformation, we assumed $J_{\mathrm{host}}(E,\Omega)=J_{\mathrm{host}}(E-\Omega)$.

[1]A. N. Gerritsen and J. O. Linde, Physica (Utrecht) **17**, 573 (1951); **18**, 877 (1951).

[2]D. Jha and M. H. Jericho, Phys. Rev. B **3**, 147 (1971); A. Nakamura and D. Kinoshita, J. Phys. Soc. Jpn. **27**, 382 (1969); **32**, 441 (1972).

[3]N. Andrei, K. Furuya, and J. H. Löwenstein, Rev. Mod. Phys. **55**, 331 (1983); J. S. Schilling, Adv. Phys. **28**, 657 (1979); G. Grüner and A. Zawadowski, Rep. Prog. Phys. **37**, 1497 (1974); J. A. Mydosh, J. Phys. Soc. Jpn. **52**, 585 (1983); A. J. Heeger, in *Solid State Physics*, edited by F. Seitz and D. Turnbull (Academic, New York, 1969), Vol. 23, p. 283; **23**, 283 (1969); F. Kondo, *ibid.*, p. 183.

[4]C. Kittel, in *Solid State Physics*, edited by F. Seitz and D. Turnbull (Academic, New York, 1968), Vol. 22; M. A. Ruderman and C. Kittel, Phys. Rev. **96**, 99 (1954); T. Kasuya, Prog. Theor. Phys. **16**, 45 (1956); K. Yosida, Phys. Rev. **106**, 893 (1957).

[5]J. R. Schrieffer and P. A. Wolff, Phys. Rev. **149**, 491 (1966); J. R. Schrieffer, J. Appl. Phys. **38**, 1143 (1967); see, however, L. L. Hirst [Z. Phys. **244**, 230 (1971)] for a remark on a factor-of-2 in error in the latter reference.

[6]P. W. Anderson, Phys. Rev. **124**, 41 (1961).

[7]E. Antonides and G. A. Sawatzky, in *Transition Metals*, edited by M. J. G. Lee, J. M. Perz, and E. Fawcett (IOP, Bristol, 1978), p. 134 (IOP Conf. Proc. No. 39).

[8]M. Vos, D. van der Marel, and G. A. Sawatzky, Phys. Rev. B **29**, 3073 (1984).

[9]D. van der Marel, G. A. Sawatzky, and F. U. Hillebrecht, Phys. Rev. Lett. **53**, 206 (1984); J. C. Fuggle, P. Bennett, F. U. Hillebrecht, A. Lenselink, and G. A. Sawatzky, *ibid.* **49**, 1787 (1982). Also see Ref. 7.

[10]A. F. J. Morgownik and J. A. Mydosh, Solid State Commun. **47**, 321 (1983); C. M. Hurd, J. Phys. Chem. Solids **30**, 539 (1969); A. K. Majumdar, V. Oestreich, and D. Wechsenfelder, Solid State Commun. **45**, 907 (1983); M. Hanson, J. Phys. **8**, 1225 (1978).

[11]J. C. Slater, *Quantum Theory of Atomic Structure* (McGraw-Hill, New York, 1960), p. 492.

[12]J. B. Mann, Los Alamos Scientific Laboratory Report No. LASL-3690 (1967) (unpublished).

[13]A. J. Bosch, J. Phys. E **17**, 1187 (1984); Ph.D. thesis, University of Gröningen, 1982.

[14]F. U. Hillebrecht (unpublished).

[15]The *Cu*Mn samples were kindly supplied by Professor J. A.

Mydosh, for which we want to express our gratitude.

[16]E. Dartyge and A. Fontaine, J. Phys. F **14**, 721 (1984).
[17]H. Bouchiat, Phys. Rev. B **23**, 1375 (1981).
[18]A. F. J. Morgownik and J. A. Mydosh, Solid State Commun. **47**, 325 (1984).
[19]H. Höchst, P. Steiner, and S. Hüffner, Z. Phys. B **38**, 201 (1980); P. T. Andrews and C. E. Johnson, Phys. Lett. **70A**, 140 (1979).
[20]A. R. Miedema, Z. Metallkdn. **69**, 455 (1978).
[21]A. D. McLachlan, J. G. Jenkin, R. C. G. Leckey, and J. Liesegang, J. Phys. F **5**, 2415 (1975).
[22]J. L. Gardner and J. A. R. Samson, J. Electron Spectrosc. Relat. Phenom. **6**, 53 (1975).
[23]D. van der Marel, G. A. Sawatzky, and J. A. Julianus, J. Phys. F **14**, 281 (1984).
[24]The effect of removing an atom equals the limit $\Delta \rightarrow \infty$ in Eq. (17). Thus, $\Delta\rho = \pi^{-1}\mathrm{Im}(\partial/\partial\omega)[\ln g(\omega)]$.
[25]D. van der Marel, G. A. Sawatzky, R. Zeller, F. U. Hillebrecht, and J. C. Fuggle, Solid State Commun. **50**, 47 (1984).
[26]A. M. Clogston, B. T. Matthias, M. Peter, H. J. Williams, E. Corenzwit, and R. J. Sherwood, Phys. Rev. **125**, 541 (1962).
[27]N. J. Shevchik, Phys. Rev. B **16**, 3428 (1977).
[28]N. V. Smith, Phys. Rev. B **3**, 1862 (1971); **9**, 1365 (1974).
[29]P. J. Braspennig, R. Zeller, A. Lodder, and P. H. Dederichs, Phys. Rev. B **29**, 703 (1984).
[30]H. P. Meyers, L. Wallden, and A. Karlson, Philos. Mag. **18**, 725 (1968).
[31]J. D. Cohen and C. P. Slichter, Phys. Rev. Lett. **40**, 129 (1978).
[32]M. C. Muñoz, B. L. Gyorffy, and K. Verhuyk, J. Phys. F **13**, 1847 (1983).
[33]T. V. Ramakrishan, in *Valence Fluctuations in Solids,* edited by L. M. Falicov, W. Hanke, and M. B. Maple (North-Holland, Amsterdam, 1981), p. 13; P. W. Anderson, *ibid.*, p. 451.